

# Coherent coupling of a superconducting flux-qubit to an electron spin ensemble in diamond

Xiaobo Zhu,<sup>1</sup> Shiro Saito,<sup>1</sup> Alexander Kemp,<sup>1</sup> Kosuke Kakuyanagi,<sup>1</sup> Shin-ichi Karimoto,<sup>1</sup> Hayato Nakano,<sup>1</sup> William J. Munro,<sup>1</sup> Yasuhiro Tokura,<sup>1</sup> Mark S. Everitt,<sup>2</sup> Kae Nemoto,<sup>2</sup> Makoto Kasu,<sup>1</sup> Norikazu Mizuochi,<sup>3,4</sup> and Kouichi Semba<sup>1,\*</sup>

<sup>1</sup>*NTT Basic Research Laboratories, NTT Corporation,*

*3-1 Morinosato-Wakamiya, Atsugi, Kanagawa 243-0198, Japan*

<sup>2</sup>*National Institute of Informatics, 2-1-2 Hitotsubashi, Chiyoda-ku, Tokyo-to 101-8430, Japan*

<sup>3</sup>*University of Osaka, Graduate school of Engineering Science,*

*1-3, Machikane-yama, Toyonaka, Osaka, 560-8531, Japan*

<sup>4</sup>*PRESTO JST, 4-1-8 Honcho, Kawaguchi, Saitama 332-0012, Japan*

(Dated: October 21, 2018)

Electron-spin nitrogen-vacancy color centers in diamond are a natural candidate to act as a quantum memory for superconducting qubits because of their large collective coupling and long coherence times. We report here the first demonstration of strong coupling and coherent exchange of a single quantum of energy between a flux-qubit and an ensemble of nitrogen-vacancy color centers.

During the last decade, research into superconducting quantum bits (qubits) based on Josephson junctions has made rapid progress [1]. Many foundational experiments have been performed [2–10] and superconducting qubits are now considered one of the most promising systems for quantum information processing. However, the experimentally reported coherence times are likely to be insufficient for future large scale quantum computation. A natural solution is a dedicated *engineered* quantum memory based on atomic and molecular systems. Since macroscopic quantum coherence was first demonstrated in Josephson junction circuits [2], the question of whether or not coherent quantum coupling between a single macroscopic artificial atom and an ensemble of natural atoms or molecules is possible has attracted significant attention [11–14]. In this letter we present for the first time evidence of coherent strong coupling between a single macroscopic superconducting artificial atom (a flux qubit) and an ensemble of electron-spin nitrogen-vacancy color centers (NV<sup>-</sup> centers) in diamond. Furthermore, we have observed coherent exchange of a single quantum of energy between a flux qubit and a macroscopic ensemble consisting of  $\sim 3 \times 10^7$  of NV<sup>-</sup> centers. This provides a foundation for future quantum memories and hybrid devices coupling microwave and optical systems.

With the early successes of single atom quantum state manipulation [15], research in quantum information processing with atomic and solid-state systems has progressed largely in a separate fashion. In recent years, significant effort has been devoted to coupling atomic and molecular system to solid-state qubits to form hybrid quantum devices [11–13]. Hybrid devices involving the integration of an atomic system with a superconducting transmission line resonator have been realized [16–18]. Such schemes have the potential to couple superconducting solid-state qubits to optical fields via atomic systems, thus enabling quantum media conversion. The

coupling strength  $g$  of an individual atomic system to one electromagnetic mode in a resonator circuit is usually too small for the coherent exchange of quantum information. However, the coupling strength of an ensemble of  $N$  such atomic systems will be enhanced by a factor of  $\sqrt{N}$  [19], allowing one to reach the strong coupling regime ( $g\sqrt{N} \gg \kappa, \gamma$ , where  $\kappa$  and  $\gamma$  are the damping rates of resonator circuit and atomic system).

Of the many possible hybrid systems, coupling a flux-qubit to an (NV<sup>-</sup>) center in diamond is particularly appealing. Firstly, the magnetic coupling between a flux-qubit and a single NV<sup>-</sup> center can be three orders of magnitude larger than that associated with a superconducting transmission line resonator [14]. Second, the ground state of an NV<sup>-</sup> center is a spin 1 triplet due to its  $C_{3v}$  symmetry (Figure 1b). The  $S = 1$  spin triplet  $|m_s = 0\rangle$  state is separated by 2.88 GHz from the near degenerate excited states  $|m_s = \pm 1\rangle$  under zero magnetic field (Figure 1c). This energy separation is ideal for a gap tunable flux-qubit to be brought on and off resonance with it.

In this Letter, we report on the first observation of vacuum Rabi oscillations between a flux-qubit and an ensemble of approximately three million NV<sup>-</sup> centers in diamond. This demonstrates strong coherent coupling between two dissimilar quantum systems with an effective collective coupling constant of  $g_{\text{ens}} \sim 70$  MHz.

We begin by describing our experimental setup as depicted in (Figure 1). An NV<sup>-</sup> diamond sample was prepared by ion implantation of  $^{12}\text{C}^{2+}$  at 700 keV under high vacuum into high-pressure, high-temperature (HPHT)-synthesized type Ib (001) surface orientation single crystal diamond. The  $^{12}\text{C}^{2+}$  ions, with a dose condition of  $3 \times 10^{13} \text{ cm}^{-2}$ , were stopped at a depth of  $600_{-100}^{+50}$  nm. This generated on the order of  $5 \times 10^{18} \text{ cm}^{-3}$  vacancies over a depth of  $\sim 0.7 \mu\text{m}$ . After implantation, the crystals were annealed at  $900^\circ\text{C}$  under vacuum for 3 hours. This high dose carbon implantation method en-

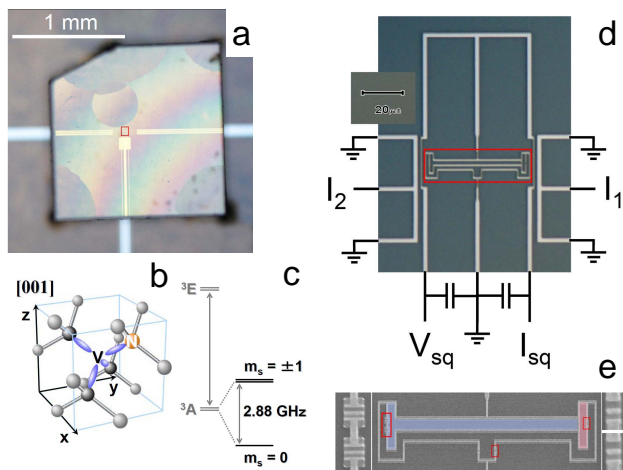


FIG. 1. **Experimental set-up of an NV-diamond sample attached to a flux-qubit system.**

(a) A diamond crystal is glued on top of a flux-qubit and its superconducting circuits (under the red box) with the diamonds  $^{12}\text{C}$  implanted (001) surface facing the chip. The distance between the flux-qubit and surface of the diamond crystal is carefully adjusted to be less than a micrometer using 100 nm height mesa structure on the diamond surface, a circle adjacent to the red square, and the optical interference pattern (Newton's ring). (b) A sketch of a NV color center of diamond with its vacancy (V) and nitrogen (N) atom, as well neighboring carbon atoms. Four equivalent NV-axis exist depicted in purple color dangling bonds, all making the same angle with [001] direction to which the magnetic field generated by the flux-qubit points. (c) Energy diagram of the NV center, with the spin triplet  $|m_s = 0\rangle$  ground state separated by 2.88 GHz from the degenerated  $|m_s = \pm 1\rangle$  excited states under zero magnetic field[28]. (d) Optical micrograph and the circuit scheme of the aluminum made flux-qubit, the magnified view of the chip under the red box region shown in Fig.1a. The central M shaped circuit contains a flux-qubit and a SQUID detector. Two high-bandwidth (20 GHz) MW-control lines located both sides of the qubit circuit. (e) The H-shaped gap tunable flux-qubit and the edge-shared SQUID used as a switching qubit state detector. The flux-qubit contains two loops, the main loop (blue) and the  $\alpha$ -control loop (magenta) which controls tunneling energy gap of the flux-qubit. Magnified view of Josephson junctions are also shown. The mutual inductance of control line-1 to the  $\alpha$ -loop and main loop are 90 fH and 256 fH, and those of control line-2 are 0.5 fH and 549 fH. The magnetic flux penetrating these two loops can be controlled in ns time scale by applying synchronized current pulses to these control lines in situ.

hances the yield of generated  $\text{NV}^-$  centers [20]. Photoluminescence (PL) optical spectroscopy (shown in Figure 2) established that  $\text{NV}^-$  centers were generated with a density of  $\sim 1.1 \times 10^{18} \text{ cm}^{-3}$  over a  $1 \mu\text{m}$  depth. We can describe the ground state of a single  $\text{NV}^-$  center by the Hamiltonian [21],

$$H_{\text{NV}} = hDS_z^2 + hE(S_x^2 - S_y^2) + hg_{\text{NV}}\mu_B \mathbf{B} \cdot \mathbf{S}, \quad (1)$$

where  $S_x, S_y, S_z$  are the usual Pauli spin 1 operators,  $D$

the zero-field splitting (2.878 GHz),  $E$  the strain-induced splitting ( $< 1$  MHz), the N-V Landé factor  $g_{\text{NV}} = 2$ , and  $\mu_B = 14 \text{ MHz/mT}$ . The last term represents the Zeeman splitting, which is negligible in our case as the magnetic field applied perpendicular to the surface of the chip to prepare the flux qubit is less than 0.1 mT.

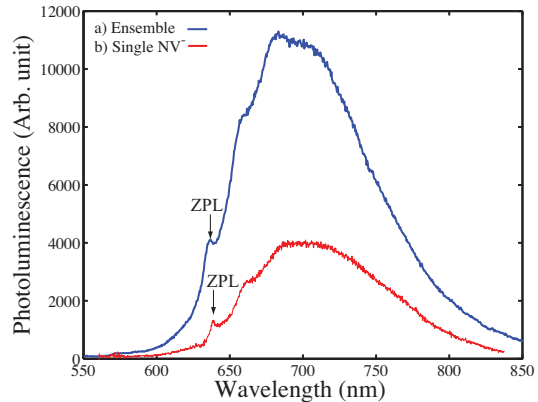


FIG. 2. **Photoluminescence spectra** of (a) ensembles of color centers in the highly carbon implanted sample and (b) a single NV- center in pure diamond at room temperature. Their signal intensities are normalized for the comparison of the spectra. In the spectrum of the single NV center, the contributions of phonon Raman scattering from bulk diamond at 573 and between 600 and 620 nm are subtracted[29]. The zero phonon line of NV- at 637 nm[29, 30] is clearly observed in both spectra. Broad spectrum of phonon replicas is also very similar to each other and to the reported ones[29, 30]. These indicate that the NV- center is produced as a major color center in the highly carbon implanted sample. The signal intensity of the ensemble is about  $6.5 \times 10^4$  times stronger than that of the single one. From this result, the concentration of the NV- center in the highly carbon implanted sample was estimated to be  $1.1 \times 10^{18} \text{ cm}^{-3}$ .

A diamond crystal was glued on top of the superconducting circuit with the  $^{12}\text{C}$  implanted surface facing the flux-qubit (Figure 1a). We used a gap tunable flux-qubit [22, 23] (Figure 1d, 1e) where the smallest junction of the three Josephson junction qubit is replaced by a low inductance superconducting quantum interference device (dc-SQUID) loop (the magenta loop in Figure 1e). The flux qubit - NV ensemble coupled system is measured by the qubit state using a built-in dc-SQUID (the biggest loop in Fig.1e sharing edges with the flux-qubit) which is inductively coupled to the qubit. When biasing the main loop close to half a flux quantum, the device is an effective two-level system [24] described by the Hamiltonian

$$H_{\text{qb}} = \frac{h}{2} (\Delta \sigma_x + \epsilon \sigma_z), \quad (2)$$

which is given in the basis of clockwise and counter-clockwise currents. Here,  $\sigma_{x,z}$  are the Pauli spin  $\frac{1}{2}$  matrices,  $h\epsilon = 2I_{\text{P}}(\Phi_{\text{ex}} - 3\Phi_0/2)$  is the energy bias ( $I_{\text{P}} \approx 300$

nA is the persistent current in the qubit,  $\Phi_{\text{ex}}$  is the external flux threading the qubit loop, and  $\Phi_0 = h/2e$  is the flux quantum), and  $\Delta$  is the tunnel splitting. The energy splitting of the gap tunable flux-qubit is  $hF = h\sqrt{\epsilon^2 + \Delta^2}$  where  $\epsilon$  and  $\Delta$  can be controlled independently by the external magnetic flux threading the two loops. This type of flux-qubit can be tuned into resonance with an  $\text{NV}^-$  ensemble in-situ at a base temperature of  $\sim 12$  mK while keeping the qubit at its optimum flux bias (degeneracy point). The total Hamiltonian of the coupled system is

$$\begin{aligned}
 H = & \frac{h}{2}(\Delta\sigma_x + \epsilon\sigma_z) \\
 & + h \sum_i [DS_{z,i}^2 + E(S_{x,i}^2 - S_{y,i}^2)] \\
 & + \frac{h}{2} \sum_i g_i\sigma_z S_{x,i},
 \end{aligned} \tag{3}$$

where  $i$  runs over the  $\text{NV}^-$  centers which couple to the flux qubit. The corresponding coupling constant can be estimated using the Biot-Savart law at  $g_i \sim 8.8$  kHz. In our situation here, the  $|\pm 1\rangle_i$  states of the  $\text{NV}^-$  electronic spin are near degenerate and so our flux-qubit couples to both the  $|0\rangle_i \rightleftharpoons |1\rangle_i$  and  $|0\rangle_i \rightleftharpoons |-1\rangle_i$  transitions. This results in an effective coupling constant  $\sqrt{2}g_i$  larger than generally anticipated.

From the spectroscopic measurements, a clear anti-crossing was observed (Figure 3a) near the degeneracy point of the flux-qubit, while no gap was observed in the same flux-qubit prior to the mounting of the ensemble (inset in Figure 3a). We also note a narrow resonance at 2.878 GHz of less than 1 MHz width near these anti-crossings. This can be ascribed to the near degenerate excited states of the  $\text{NV}^-$  ensemble and so indicates a strain-induced zero-field splitting coefficient  $E$  of less than 1 MHz. From the fine scan spectroscopy shown in (Figure 3b), a vacuum Rabi splitting near  $g_{\text{ens}} \sim 70$  MHz was clearly observed confirming strong coupling between the flux-qubit and the  $\text{NV}^-$  ensemble. Next from the measured vacuum Rabi splitting and our calculated value of  $g_i$  we can estimate the number of  $\text{NV}^-$  centers in the ensemble at  $N = g_{\text{ens}}^2/2g^2 \approx 3.2 \times 10^7$ , where the factor of 2 in the denominator is due to the two-fold degeneracy of the excited  $|\pm 1\rangle_i$  states of an  $\text{NV}^-$  center. This estimate is consistent with the density of  $\text{NV}^-$  centers measured by PL spectroscopy in the whole sample ( $1.1 \times 10^{18} \text{ cm}^{-3}$ ) multiplied by the volume of centers coupling to the flux qubit (area  $40 \mu\text{m}^2 \times$  effective thickness  $0.7 \mu\text{m}$ ). The PL spectroscopy approach gives the number of coupled centers as  $\approx 3.1 \times 10^7$ .

Next, we investigated the dynamics of our system in the time domain using a similar measurement cycle to that performed in qubit-LC resonator coupled systems [25]. We first excited the flux-qubit and then brought it into resonance with the  $\text{NV}^-$  ensemble. Single energy

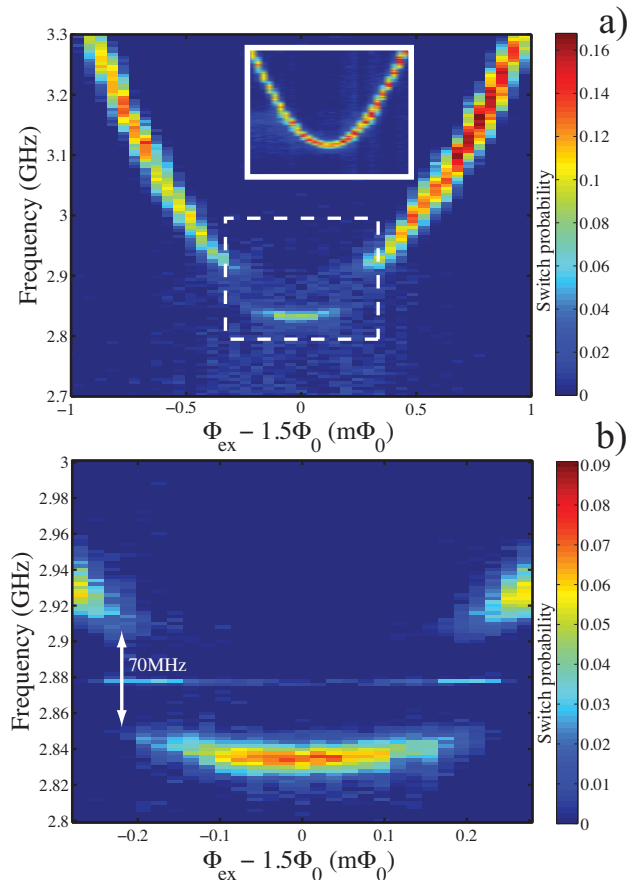


**FIG. 3. Energy spectrum of the flux-qubit coupled to ensemble of NV-centers.** a) Resonant frequencies indicated by peaks in the SQUID detector switching probability when a 500 ns long microwave pulse excites the system before the readout pulse. Data are represented as a function of the external magnetic flux through the effective qubit area ( $\Phi_{\text{ex}} = \Phi_m + \Phi_\alpha/2$ , where  $\Phi_m$  and  $\Phi_\alpha$  are the flux through the qubit main-loop and  $\alpha$ -loop, respectively). Inset: resonant frequency spectrum of the same flux-qubit over the same region without mounting the NV-diamond crystal. (b) Magnified view of the white dotted box region in (a). A vacuum Rabi splitting as large as 70 MHz is clearly observed. Since the qubit phase relaxation time measured by spin-echo  $T_2^{\text{echo}} \approx 0.25 \mu\text{s}$ , the strong coupling condition is satisfied by the  $\sqrt{N}$  enhancement in  $g$ .  $N \approx 3 \times 10^7$  is the estimated number of electron spins in the ensemble strongly coupled to the flux-qubit.

quantum exchange between the flux-qubit and  $\text{NV}^-$  ensemble at resonance manifests itself as the vacuum Rabi oscillations

$$|1\rangle_{\text{qb}}|0\rangle_{\text{ens}} \rightleftharpoons |0\rangle_{\text{qb}}|1\rangle_{\text{ens}} \tag{4}$$

where  $|1\rangle_{\text{ens}} = \frac{1}{\sqrt{N}} \sum_i S_{+,i} |00 \dots 0\rangle$ , with  $S_{+,i} = |1\rangle_i \langle 0|_i + |-1\rangle_i \langle 0|_i$  being the raising operator of the  $i$ -th  $\text{NV}^-$  spin to both the  $|\pm 1\rangle$  states. (Figure 4a) clearly shows vacuum Rabi oscillations between the flux-qubit

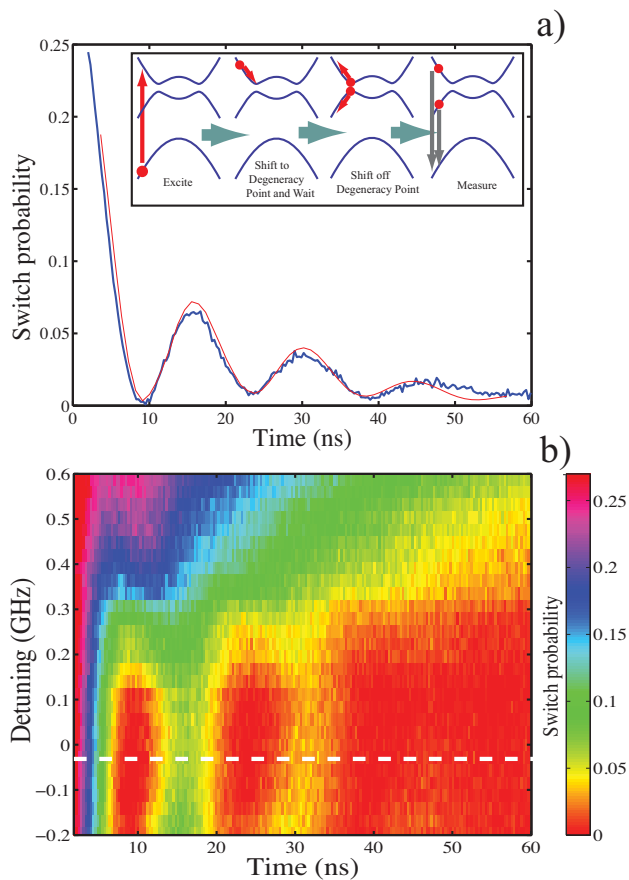


FIG. 4. **Vacuum Rabi oscillation of the flux-qubit NV-ensemble coupled system.** (a) Damped oscillation (blue curve) of an initially excited flux coupled to an NV-ensemble with the results from a phenomenological model shown as a thin red curve. Inset, schematic measurement sequence for the vacuum Rabi measurement. An Initial ground state  $|0\rangle_{\text{qubit}}|0\rangle_{\text{ens}}$  is prepared by letting the system to relax longer than  $800 \mu\text{s}$  under the base temperature ( $T=12 \text{ mK}$ ) of the dilution refrigerator at the optimal readout flux bias. Immediately following this a  $\pi$ -pulse is applied to the flux qubit resulting in the state  $|1\rangle_{\text{qubit}}|0\rangle_{\text{ens}}$ . The system is then brought into resonance non-adiabatically by a flux-bias shift current pulse through the control line 2. On resonance vacuum Rabi oscillation takes place for a given time;  $|1\rangle_{\text{qubit}}|0\rangle_{\text{ens}} \rightleftharpoons |0\rangle_{\text{qubit}}|1\rangle_{\text{ens}}$ . Finally, the SQUID detector reads the qubit state as a function of the time keeping the system on resonance. We repeat these measurement typically  $2 \times 10^4$  times under the same condition to obtain good statistics. (b) 2D plot of the SQUID detector switching probability as a function of both the detuning by flux bias shift and the time keeping the flux-qubit NV-ensemble system at a given detuning. The white broken line corresponds to the switching probability shown in a).

and ensemble of electronic spins at the 2.878 GHz resonance. The decay time of the oscillations however is approximately 20 ns. This is much shorter than the relaxation time of both the flux-qubit ( $T_{1,\text{qb}} \sim 150 \text{ ns}$ )

and the NV<sup>-</sup> ensemble ( $T_{1,\text{NV}} \gg 10 \mu\text{s}$ ). As we tune the flux-qubit away from the 2.878 GHz resonance, the decay time associated with vacuum Rabi measurement becomes significantly longer (Figure 4b). From these results, one must conclude that a source of strong dephasing of unknown origin exists in the system near resonance. There are several likely sources. The most probable is a large electron spin  $\frac{1}{2}$  bath from the P1 (nitrogen atom substituting a carbon atom) centers present in our HPHT Ib-type diamond crystal used to prepare the NV<sup>-</sup> ensemble. In our situation, where there is no external magnetic field, the NV<sup>-</sup> centers and P1 centers naturally couple[14]. Hanson et. al [26] have shown an enhanced decay may result. The P1 center issue can be eliminated to a large extent by applying an external magnetic field to split the  $|\pm 1\rangle$  NV<sup>-</sup> states. A 1 mT field could split these by approximately 15 MHz, detuning the P1 centers and thus significantly improving the dephasing time of the coupled system. We can also decrease the number of P1 centers in the sample (from 100 ppm to 1 ppm) by using different synthesized diamond crystals. In addition, by using non HPHT Ib-type crystals we can remove the effect of other natural defects that may be present. Finally there is also a strong hyperfine interaction ( $\sim 100 \text{ MHz}$ ) between the NV<sup>-</sup> electron spin and  $^{13}\text{C}$  nuclear spins. Without the nuclear spins being initially polarized, unwanted dephasing will result. By polarizing the nuclear spins this source of dephasing can be removed. This should allow us to observe vacuum Rabi oscillations where we are limited by  $T_2$  of the flux-qubit.

In conclusion, we have experimentally demonstrated strong coherent coupling between a flux-qubit and an ensemble of nitrogen-vacancy color centers in single crystal diamond. Furthermore, we have observed, via vacuum Rabi oscillations, the coherent exchange (transfer) of a single quantum of energy. This is the first step towards the realization of a long lived quantum memory for condensed matter systems with an additional potential future application as an interface between the microwave and optical domains.

*Acknowledgments:* We thank T. Tawara, H. Gotoh and T. Sogawa for optical measurement in the early stage of this work. This work was supported in part by the Funding Program for World-Leading Innovative R&D on Science and Technology (FIRST), Scientific Research of Specially Promoted Research, Grant No.18001002 by MEXT, Grant-in-Aid for Scientific Research on Innovative Areas Grant No.22102502, and Scientific Research(A) Grant No.22241025 by Japanese Society for the Promotion of Science (JSPS). M.S.E. was supported with a JSPS fellowship.

\* semba.kouichi@lab.ntt.co.jp

- [1] Clarke, J. & Wilhelm, F. K. *Nature* **453**, 1031 (2008).
- [2] Nakamura, Y., Pashkin, Yu. A. & Tsai, J. S. *Nature* (London) **398**, 786 (1999).
- [3] Vion, D., Aassime, A., Cottet, A., Joyez, P., Pothier, H., Urbina, C., Esteve, D. & Devoret, M. H. *Science* **296**, 886 (2002).
- [4] Chiorescu, I., Nakamura, Y., Harmans, C. J. P. M. & Mooij, J. E. *Science* **299**, 1869 (2003).
- [5] Sillanpää, M. A., Park, J. I. & Simmonds, R. W. *Nature* **449**, 438 (2007).
- [6] Majer, J., Chow, J. M., Gambetta, J. M., Koch, J., Johnson, B. R., Schreier, J. A., Frunzio, L., Schuster, D. I., Houck, A. A., Wallraff, A., Blais, A., Devoret, M. H., Girvin, S. M. & Schoelkopf, R. J. *Nature* **449**, 443 (2007).
- [7] DiCarlo, L., Chow, J. M., Gambetta, J. M., Bishop, L. S., Johnson, Schuster, D. I., Majer, J., Blais, A., Frunzio, L., Girvin, S. M. & Schoelkopf, R. J. *Nature* **460**, 240 (2009).
- [8] Ansmann, M., Wang, H., Bialczak, R. C., Hofheinz, M., Lucero, E., Neeley, M., O'Connell, A. D., Sank, D., Weides, M., Wenner, J., Cleland, A. N. & Martinis, J. M. *Nature* **461**, 504 (2009).
- [9] Neeley, M., Bialczak, R. C., Lenander, M., Lucero, E., Mariantoni, M., O'Connell, A. D., Sank, D., Wang, H., Weides, M., Wenner, J., Yin, Y., Yamamoto, T., Cleland, A. N. & Martinis, J. M. *Nature* **467**, 570 (2010).
- [10] DiCarlo, L., Reed, M. D., Sun, L., Johnson, B. R., Chow, J. M., Gambetta, J. M., Frunzio, L., Girvin, S. M., Devoret, M. H. & Schoelkopf, R. J. *Nature* **467**, 574 (2010).
- [11] Sørensen, Anders S., van der Wal, Caspar H., Childress, Lilian I. & Lukin, Mikhail D. *Phys. Rev. Lett.* **92**, 063601 (2004).
- [12] Tian, L., Rabl, P., Blatt, R. & Zoller, P. *Phys. Rev. Lett.* **92**, 247902 (2004).
- [13] Rabl, P., DeMille, D., Doyle, J. M., Lukin, M. D., Schoelkopf, R. J. & Zoller, P. *Phys. Rev. Lett.* **97**, 033003 (2006).
- [14] Marcos, D., Wubs, M., Taylor, J. M., Aguado, R., Lukin, M. D. & Sørensen, A. S. *Phys. Rev. Lett.* **105**, 210501 (2010).
- [15] Brune, M., Schmidt-Kaler, F., Maali, A., Dreyer, J., Hægley, E., Raimond, J. M. & Haroche, S. *Phys. Rev. Lett.* **76**, 1800 (1996).
- [16] Schuster, D. I., Sears, A. P., Ginossar, E., DiCarlo, L., Frunzio, L., Morton, J. J. L., Wu, H., Briggs, G. A. D., Buckley, B. B., Awschalom, D. D. & Schoelkopf, R. J. *Phys. Rev. Lett.* **105**, 140501 (2010).
- [17] Kubo, Y., Ong, F. R., Bertet, P., Vion, D., Jacques, V., Zheng, D., Dréau, A., Roch, J.-F., Auffeves, A., Jelezko, F., Wrachtrup, J., Barthe, M. F., Bergonzo, P. & Esteve, D. *Phys. Rev. Lett.* **105**, 140502 (2010).
- [18] Amsüss, R., Koller, C., Nöbauer, T., Putz, S., Rotter, S., Sandner, K., Schneider, S., Schramböck, M., Steinhäuser, G., Ritsch, H., Schmiedmayer, J. & Majer, J. *arXiv:1103.1045*
- [19] Raizen, M. G., Thompson, R. J., Brecha, R. J., Kimble, H. J. & Carmichael, H. J. *Phys. Rev. Lett.* **63**, 240 (1989).
- [20] Naydenov, B., Richter, V., Beck, J., Steiner, M., Neumann, P., Balasubramanian, G., Achard, J., Jelezko, F., Wrachtrup, J. & Kalish, R. *Appl. Phys. Lett.* **96**, 163108 (2010).
- [21] Neumann, P., Kolesov, R., Jacques, V., Beck, J., Tisler, J., Batalov, A., Rogers, L., Manson, N. B., Balasubramanian, G., Jelezko, F. & Wrachtrup, J. *New J. Phys.* **11**, 013017 (2009).
- [22] Zhu, X., Kemp, A., Saito, S., & Semba, K. *Appl. Phys. Lett.* **97**, 102503 (2010).
- [23] Fedorov, A., Feofanov, A. K., Macha, P., Forn-Daz, P., Harmans, C. J. P. M. & Mooij, J. E. *Phys. Rev. Lett.* **105**, 060503 (2010).
- [24] Mooij, J. E., Orlando, T. P., Levitov, L., Tian, L., van der Wal, C. H. & Lloyd S. *Science* **285**, 1036, (1999).
- [25] Johansson, J., Saito, S., Meno, T., Nakano, H., Ueda, M., Semba, K. & Takayanagi, H. *Phys. Rev. Lett.* **96**, 127006 (2006).
- [26] Hanson, R., Dobrovitski, V. V., Feiguin, A. E., Gywat, O. & Awschalom, D. D. *Science* **320**, 352, (2008).
- [27] Mizuochi, N., Neumann, P., Rempp, F., Beck, J., Jacques, V., Siyushev, P., Nakamura, K., Twitchen, D., Watanabe, H., Yamasaki, S., Jelezko & F., Wrachtrup, J. *Phys. Rev.* **B80**, 041201(R) (2009).
- [28] Jelezko, F., Gaebel, T., Popa, I., Gruber, A. & Wrachtrup, J. *Phys. Rev. Lett.* **92**, 076401 (2004).
- [29] Gruber, A., Dräbenstedt, A., Tietz, C., Fleury, L., Wrachtrup, J. & von Borczyskowski, C. *Science* **276**, 2012, (1997).
- [30] Kurtsiefer, Ch., Zarda, P., Mayer, S. & Weinfurter, H. *Phys. Rev. Lett.* **85**, 290 (2000).